Modulation Schemes for Single-Phase B6 Converters With Two Asymmetrical Terminal Voltages

Qin, Zian; Loh, Poh Chiang; Blaabjerg, Frede

Published in:
I E E E Transactions on Industrial Electronics

DOI (link to publication from Publisher):
10.1109/TIE.2015.2464296

Publication date:
2016

Document Version
Accepted author manuscript, peer reviewed version

Modulation Schemes for Single-Phase B6 Converters with Two Asymmetrical Terminal Voltages

Qin, Zian; Loh, Poh Chiang; Blaabjerg, Frede;
Published in:
IEEE Transactions on Industrial Electronics

DOI (link to publication from Publisher):
10.1109/TIE.2015.2464296,

Publication date:
July 2015

Modulation Schemes for Single-Phase B6 Converters with Two Asymmetrical Terminal Voltages

Zian Qin, *Student Member*, *IEEE*, Poh Chiang Loh, and Frede Blaabjerg, *Fellow*, *IEEE*

***Abstract*—B6 converter uses six switches divided equally among three phase-legs. It has commonly been used as a three-phase rectifier or inverter, mostly under balanced conditions. Three-phase conversion is however not the only area, where B6 converter has been used. The same topology has been tried for single-phase power decoupling and single-phase ac-dc-ac conversion, where comparably lesser switches are needed. Although the basic modulation principle is still reliant on three modulating references for the three phase-legs, requirements imposed on the modulating references are different and usually asymmetrical. How these asymmetrical references should be formulated to meet various performance specifications of a single-phase B6 converter is the theme of this paper. Simulation and experimental results have been obtained for verifying the modulation schemes proposed.**

***Index Terms*—Single phase, ac-dc-ac converter, B6 converter, reduced switch converter, modulations.**

I. INTRODUCTION

Although many power converter topologies have been developed over the years, the voltage-source B6 converter has retained its importance to the industry. One of the reasons is its topological simplicity, which as indicated in Fig. 1(a), is simply three phase-legs connected in parallel, sharing a common dc-link capacitor. Each phase-leg has two switches with accompanied anti-parallel diodes. These switches cannot be turned on simultaneously to avoid shorting the dc capacitor. They should therefore be switched in complement (e.g. $S_1 = !S_2$, where ! is the logical NOT operator) except during dead-time when both switches are intentionally turned off for a short duration. This requirement and many operating issues of the B6 converter are presently well-understood, and hence less costly to adopt, as compared with a brand new topology. It is thus attractive to the industry, mostly as a three-phase converter found in motor drives [1], [2], grid interfacing converters [3], [4] and power quality conditioners [5], [6].

As a three-phase converter, the B6 converter is usually not tied to the star-point of the load or source, which in turn, allows it to be modulated differently by adding a common triplen offset to its three modulating references. The offset, when sized properly, gives rise to significant performance boosting in terms of better spectral quality, higher modulation index, lesser power losses or a combination of them [7-13]. Popular examples include offsets used with continuous centered modulation, 60°-discontinuous modulation and 30°-discontinuous modulation reviewed in [9]. The addition of offset has subsequently been demonstrated in [10] to be equivalent to the explicit space vector modulation, which certainly, is expected since it is still the switching of the same B6 converter. It is therefore possible to derive the other as long as one of them is defined.

Regardless of which method is chosen, modulation of three-phase B6 converter is presently well-established, especially under balanced terminal voltage condition. It should however be noted that B6 converter is not only used as a three-phase converter. It can also operate as a reduced-switch single-phase ac-dc-ac converter [14-16] or a single-phase converter with power ripple decoupling [17-22]. The reduced-switch ac-dc-ac B6 converter was, in fact, proposed in year 2000 for replacing two full-bridges with four phase-legs connected back-to-back. It has since been commonly cited for comparison with other reduced-switch converters proposed in [23-26], where the main concerns mentioned with the B6 converter are its more restrictive input-output frequency selection and higher dc-link voltage demanded. These concerns have limited the scope of the B6 converter as a single-phase ac-dc-ac converter, but it is still suitable for use with an uninterruptible power supply (UPS) or a power conditioner [14-16], where input and output frequencies are the same.

Another usage of the B6 converter is as a single-phase converter with power ripple decoupling [17-22]. The three phase-legs in this case are divided such that one of them is connected to the intended single-phase ac system, and another is connected to a small film capacitor. The last phase-leg is shared between the ac system and film capacitor as their common return path. Any double-line-frequency power ripple contributed by the ac system can then be diverted to the film capacitor, rather than disturbing the dc side of the converter. Placing the film capacitor in this manner has the advantage of requiring only ac fundamental voltage across the capacitor, which in general, demands a smaller capacitance and simpler control. Recent work in [22] has also shown that with proper modulation, the dc-link voltage required by the B6 converter for power ripple decoupling can be reduced, which although is important, is only one requirement out of a few that can be optimized.

Manuscript received February 7, 2015; revised June 6, 2015; accepted July 11, 2015.

The authors are with the Department of Energy Technology, Aalborg University, Pontoppidanstraede 101, Aalborg 9220, Denmark. (Email: zqi@et.aau.dk, pcl@et.aau.dk, fbl@et.aau.dk)

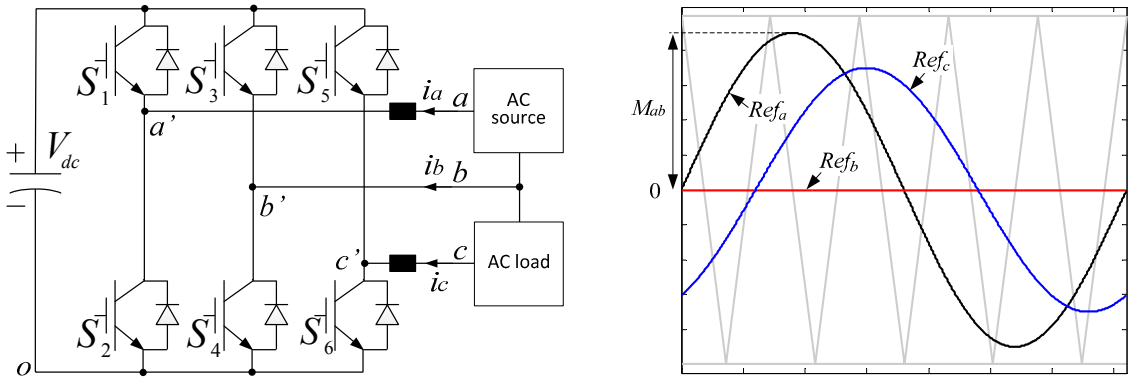

(a) (b)

Fig. 1. Illustrations of (a) single-phase B6 converter and (b) its simple reference-carrier arrangement.

It is therefore clear that the B6 converter is not only a three-phase converter. It can be used as a single-phase converter with mostly asymmetrical terminal voltage and modulation requirements. These requirements are comparably less studied, and are hence studied here to explore schemes that can minimize dc-link voltage, selected current ripple, total power loss, differences in switch thermal stresses or a combination of them. Simulation and experimental results have been obtained for validating the modulation schemes presented, before concluding the challenges resolved by them.

II. B6 Converter

The B6 converter is shown in Fig. 1(a), configured as a single-phase converter with two sets of ac terminals. The terminals can be connected to an ac source and an ac load, or a small film capacitor for power ripple decoupling. If the single-phase ac source and load are replaced by a three-phase source or load, the B6 converter then operates as a three-phase converter widely used in the industry. Whether as a single-phase or three-phase converter under unbalanced condition, terminal voltages of the B6 converter will usually be asymmetrical even though some differences still exist between them. To illustrate, the single-phase B6 converter shown in Fig. 1(a) is considered, where a shared phase-leg between the source and load can clearly be seen. Current flowing through this phase-leg is given by the sum of return currents from the source and load, which in most cases, cancel each other prominently. This cancellation is an advantage of the B6 converter, which must usually be present before the B6 converter will be considered for single-phase applications.

As a single-phase converter, the B6 converter must be modulated accordingly. The simplest reference-carrier arrangement that can be used by it is probably shown in Fig. 1(b). Expressions for the references (Ref_a, Ref_b and Ref_c) and their generated voltages (v_{ab} and v_{cb}) at the converter terminals are given in (1), where M_{ab} and M_{cb} are modulation indexes, ω_1 is the angular fundamental frequency, and φ_1 is the phase between the two generated voltages.

$$\begin{cases} Ref_a = M_{ab}sin(\omega_1 t) \\ Ref_b = 0 \\ Ref_c = M_{cb}sin(\omega_1 t + \varphi_1) \\ v_{ab} = 0.5V_{dc} \times M_{ab}sin(\omega_1 t) \\ v_{cb} = 0.5V_{dc} \times M_{cb}sin(\omega_1 t + \varphi_1) \end{cases} \quad (1)$$

The main feature of the arrangement is a simple zero reference assigned to the shared phase-leg, which will certainly help if the input and output frequencies are different. The zero reference will however burden the converter unnecessarily if the two frequencies are similar like assumed in (1). More specifically, the dc-link voltage needed by the B6 converter will be doubled that needed by two full-bridges connected back-to-back, if the arrangement shown in Fig. 1(b) is used for modulation. This doubled dc-link voltage and its accompanied higher stresses will usually render the B6 converter as unattractive even though it uses two lesser switches than the two full-bridges. The reference-carrier arrangement shown in Fig. 1(b) is therefore not recommended if the B6 converter operates with a single common frequency.

III. Continuous Modulation

A. Centered Modulation

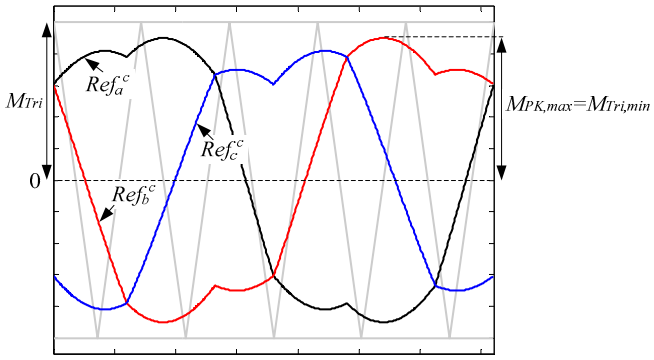

Fig. 2. Reference-carrier arrangement obtained with centered scheme.

Referring to (1) and Fig. 1(b), the relative placement of the three references, treated as a whole, within the carrier band does not have to be fixed so long as their vertical spacing and sequence produce the desired ac voltages v_{ab} and v_{cb} in (1). Their relative placement can hence be varied to create different performance advantages for the B6 converter. This is similar to the addition of triplen offset to a three-phase converter, but with asymmetry introduced. The modulation objectives expected from a single-phase B6 converter may therefore differ, even though some like keeping the converter dc-link voltage low remains unchanged. The converter dc-link voltage can indeed be minimized by centering the three references, treated as a whole, along the horizontal axis. In other words, it means the maximum and minimum references must have the same absolute magnitude, but of opposite

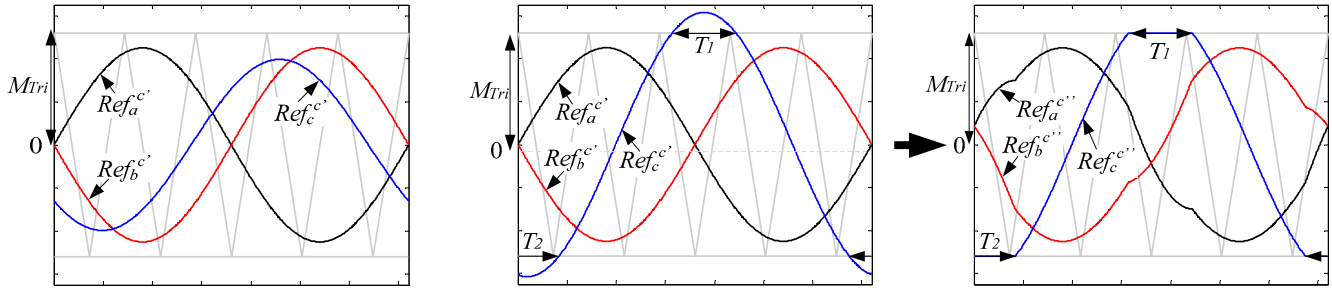

Fig. 3. Reference-carrier arrangements obtained with partially centered scheme with (a) $Ref_c^{c'} \le M_{Tri}$ and (b) $Ref_c^{c'} > M_{Tri}$.

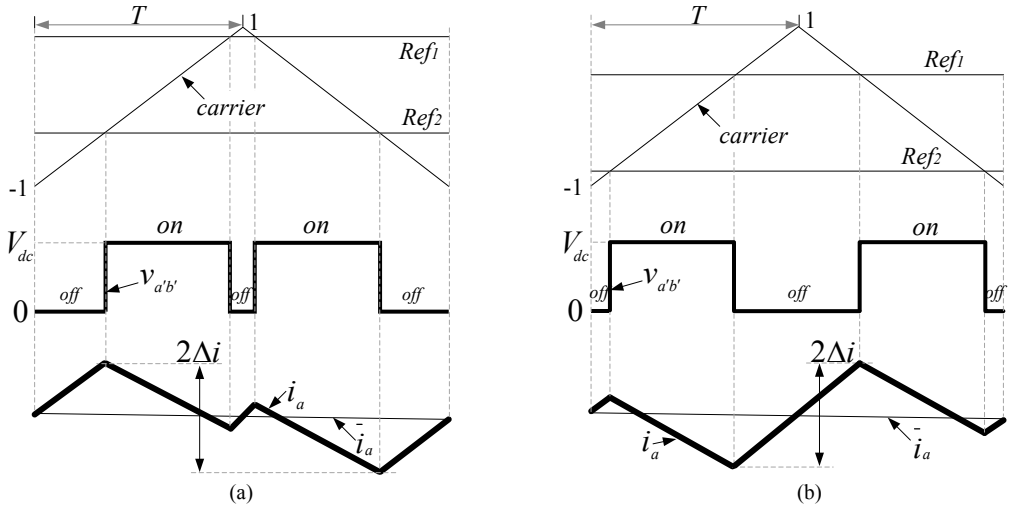

Fig. 4. Reference placements in a carrier cycle during (a) T_2 and (b) T_1.

polarity. Such placement can be realized by adding a common offset $M_{off,C1}$ to (1), to give those modified references Ref_a^C, Ref_b^C and Ref_c^C in (2).

$$\begin{cases} Ref_a^C = Ref_a + M_{off,C1} \\ Ref_b^C = Ref_b + M_{off,C1} \\ Ref_c^C = Ref_c + M_{off,C1} \\ M_{off,C1} = \\ \quad -\dfrac{[max(Ref_a, Ref_b, Ref_c) + min(Ref_a, Ref_b, Ref_c)]}{2} \end{cases} \tag{2}$$

Although $M_{off,C1}$ in (2) is similar to that used for three-phase balanced modulation, its significance is more prominent here in terms of determining the minimum dc-link voltage needed. This is unlike three-phase balanced modulation, where the minimum dc-link voltage needed is pretty obvious. To illustrate how the minimum dc-link voltage needed by the single-phase B6 converter can be determined, variations of (2) are drawn in Fig. 2, where the largest peak among the three modified references is notated as $M_{PK,max}$. Value for $M_{PK,max}$ can generally be determined using (3).

$$M_{PK,max} = max(M_{ab}, M_{cb}, M_{ac})/2 \tag{3}$$

where $0.5V_{dc} \times M_{ac}$ is the magnitude of $v_{ac} = v_{ab} - v_{cb}$ computed using ac terminal voltages defined in (1). Value of M_{ac} can further be computed using (4) based on simple geometry.

$$M_{ac} = \sqrt{M_{ab}^2 + M_{cb}^2 - 2M_{ab}M_{cb}cos\varphi_1} \tag{4}$$

To retain its linear characteristics, the carrier M_{Tri} used for comparison with the references in (2) must hence be either equal or larger than $M_{PK,max}$, which in terms of expression, is given in (5).

$$M_{Tri} \ge M_{Tri,min} = M_{PK,max} = max(M_{ab}, M_{cb}, M_{ac})/2 \tag{5}$$

where $M_{Tri,min}$ is the smallest carrier peak necessary, which in terms of basic modulation principle, is also the smallest normalized dc-link voltage needed without causing over-modulation. Centering of all three references therefore has the advantage of identifying the smallest dc-link voltage easily.

From Fig. 1(b), it is also obvious that the reduction of carrier peak achievable is the least when maximum of one reference (Ref_a or Ref_c) coincides with minimum of the other. This happens when both references in Fig. 1(b) are 180° out of phase or when they have unsynchronized frequencies (e.g. $\omega_a > \omega_c$ and $\omega_a/\omega_c \ne k$, where k is an integer, and ω_a and ω_c are different frequencies of Ref_a and Ref_c, respectively). A higher dc-link voltage is thus needed in those cases, which may shadow the reduced-switch feature of the B6 converter when used as a single-phase converter. The B6 converter is thus more likely to be used for applications with a common terminal frequency and a phase shift that permits a much smaller dc-link voltage to be used. Some possibilities are UPS, power conditioner [14-16], and converter with power ripple decoupling [17-22], as also mentioned in Section I.

B. Partially Centered Modulation

The centered modulation scheme in Section III(A) places the three references centrally within the carrier band, which for a three-phase balanced converter, is attractive since current ripples from all three phases are reduced uniformly. However,

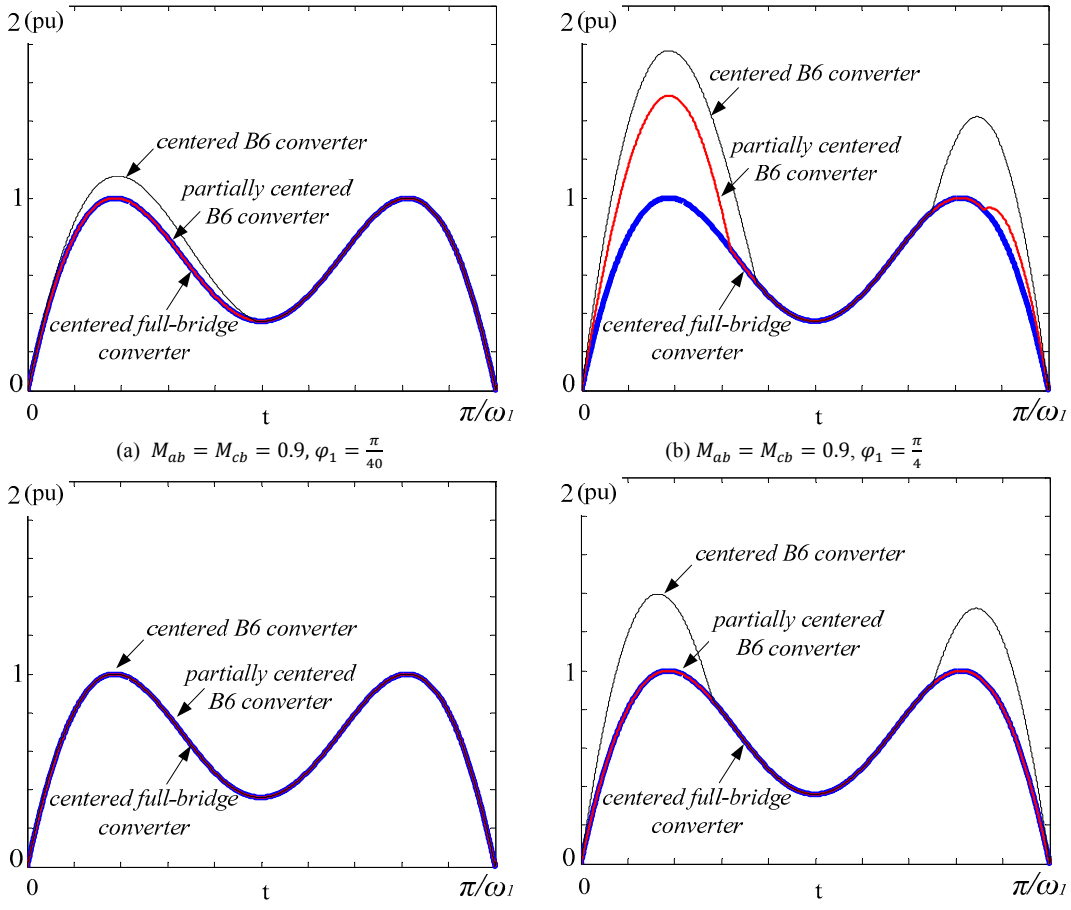

(a) $M_{ab} = M_{cb} = 0.9, \varphi_1 = \frac{\pi}{40}$ (b) $M_{ab} = M_{cb} = 0.9, \varphi_1 = \frac{\pi}{4}$

(c) $M_{ab} = 0.9, M_{cb} = 0.7, \varphi_1 = \frac{\pi}{40}$ (d) $M_{ab} = 0.9, M_{cb} = 0.7, \varphi_1 = \frac{\pi}{4}$

Fig. 5. Comparison of current ripples imposed on i_a by different modulation schemes ($1\ pu = \frac{V_{dc}T}{8L}$).

for an asymmetrical single-phase B6 converter, reducing the current ripples uniformly may not be necessary. For example, with the ac load of the single-phase B6 converter shown in Fig. 1(a) replaced by a film capacitor for power ripple decoupling, current flowing through the ac source may demand lower ripple than current flowing through the film capacitor. In that case, references for the two phase-legs tied to the source should be centered, rather than centering all three references. Such two-reference centering can be implemented by dividing the source voltage v_{ab} equally between the two references. The modified references $Ref_a^{C\prime}$, $Ref_b^{C\prime}$ and $Ref_c^{C\prime}$ then become (6), after adding the common offset $M_{off,C2}$ to (1).

$$\begin{cases} Ref_a^{C\prime} = Ref_a + M_{off,C2} \\ Ref_b^{C\prime} = Ref_b + M_{off,C2} \\ Ref_c^{C\prime} = Ref_c + M_{off,C2} \\ M_{off,C2} = -0.5 \times (Ref_a + Ref_b) \end{cases} \quad (6)$$

For the considered example, $M_{off,C2} = -0.5Ref_a = -0.5M_{ab}sin(\omega_1 t)$, which when substituted to (6), results in those two possible reference-carrier arrangements shown in Fig. 3(a) and (b). In both figures, the carrier peak is marked as M_{Tri}, which in theory, will have the same minimum value $M_{Tri,min}$ given in (5). In practice, a small safety margin may however be added to $M_{Tri,min}$ for avoiding over-modulation. This is strictly a recommendation rather than a necessary requirement.

The eventual carrier peak chosen is found to be large enough in Fig. 3(a) for confining all references within the carrier band. Fig. 3(a) therefore does not require further modification. On the other hand, the left diagram in Fig. 3(b) has a reference $Ref_c^{C\prime}$ exceeding the carrier band during T_1 and T_2. It is therefore not immediately applicable. Instead, the three references during T_1 must be shifted down equally until the modified $Ref_c^{C\prime\prime}$ clamps to the carrier peak like shown in the right diagram of Fig. 3(b). Further downward shifting is also possible, but will worsen the centering of the modified $Ref_a^{C\prime\prime}$ and $Ref_b^{C\prime\prime}$ within the carrier band. It is therefore not encouraged if the objective is to minimize current ripple from those phase-legs modulated by $Ref_a^{C\prime\prime}$ and $Ref_b^{C\prime\prime}$. The same shifting must be applied during T_2, but instead of shifting down, the references must be shifted up until $Ref_c^{C\prime\prime}$ clamps to the carrier trough. With the shifting included, (6) changes to (7), where the additional offset introduced for shifting is notated as $M_{off,C3}$.

$$\begin{cases} Ref_a^{C\prime\prime} = Ref_a^{C\prime} + M_{off,C3} \\ Ref_b^{C\prime\prime} = Ref_b^{C\prime} + M_{off,C3} \\ Ref_c^{C\prime\prime} = Ref_c^{C\prime} + M_{off,C3} \end{cases}$$

$$M_{off,C3} = \begin{cases} 0, & if\ (Ref_a^{C\prime}, Ref_b^{C\prime}, Ref_c^{C\prime}) \le M_{Tri} \\ sgn(Ref_c^{C\prime}) * M_{Tri} - Ref_c^{C\prime}, & if\ |Ref_c^{C\prime}| > M_{Tri} \end{cases}$$
$$M_{Tri} \ge M_{Tri,min} \quad (7)$$

where *sgn*() is a function for returning the polarity of parameter enclosed by its parentheses.

To demonstrate the reduction of current ripple, mathematical formulation can be derived from those terminal

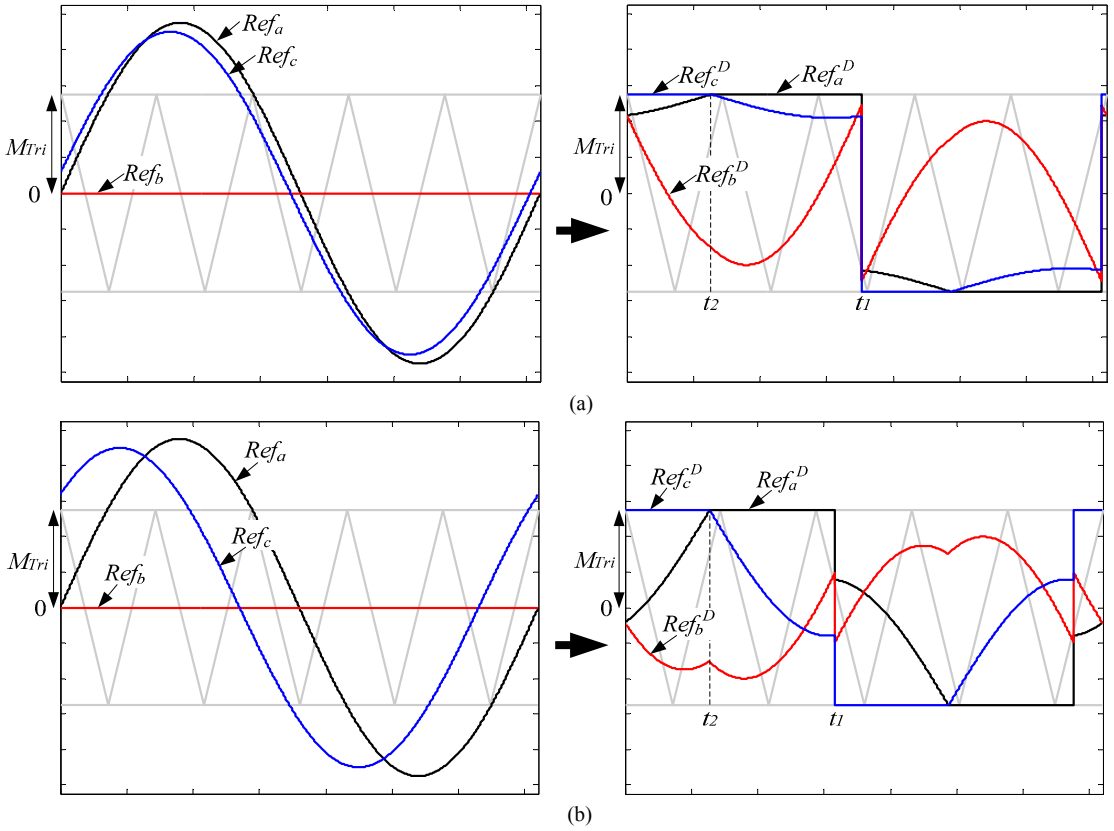

Fig. 6. Reference-carrier arrangements obtained with the discontinuous scheme when (a) v_{ab} and v_{cb} are close in magnitude and phase, and (b) $\varphi_1 = \pi/4$.

pulse voltage and current waveforms shown in Fig. 4(a) and (b) for the assumed example. In those figures, Ref_1 and Ref_2 are for representing either $Ref_a^{C''}$ or $Ref_b^{C''}$, depending on which is higher at the instant of consideration. They are shifted up like in Fig. 4(a) when in interval T_2, and shifted down like in Fig. 4(b) when in interval T_1. Their respective peak current ripple Δi expressions can then be derived as (8) and (9), where T and L represent the half carrier period and ac filter inductance, respectively.

$$L \times 2|\Delta i| = \frac{Ref_2+1}{2} \times 2T \times |v_{ab}| \quad (8)$$

$$L \times 2|\Delta i| = \frac{1-Ref_1}{2} \times 2T \times |v_{ab}| \quad (9)$$

Noting further that $Ref_1 \geq Ref_2$, (8) and (9) can be combined to give the general current ripple expression in (10).

$$|\Delta i| = max(min(Ref_a^{C''}, Ref_b^{C''}) + 1, 1 - max(Ref_a^{C''}, Ref_b^{C''})) \times \frac{T}{2L} \times |v_{ab}| \quad (10)$$

References from (7) can subsequently be substituted to (10) for computing the peak current ripple expected from the partially centered scheme. The same expression in (10) can also be used for computing current ripple expected from the centered scheme by simply replacing $Ref_a^{C''}$ and $Ref_b^{C''}$ with Ref_a^{C} and Ref_a^{C} from (2). The obtained current ripples are plotted in Fig. 5, together with ripple expected from a full-bridge converter, operating under the same ac and dc conditions. Comparison with the full-bridge converter is meaningful since the single-phase B6 converter has always been cited as the reduced-switch version of two full-bridges connected back-to-back. It ripple value is therefore included in Fig. 5, which is clearly the lowest since condition like $Ref_c^{C'}$ exceeding the carrier in Fig. 3(b) will not occur.

The condition in Fig. 3(b) must however be rectified when used with the partially centered B6 converter. Its current ripple drawn from the ac source is therefore higher than the full-bridge converter during T_1 and T_2 of the fundamental cycle. Length of T_1 and T_2, and the difference in ripple magnitude depend on the relative magnitude (M_{ab}: M_{cb}) and phase-shift φ_1 of the two ac voltages v_{ab} and v_{cb}. For example, in Fig. 5(a) and (c), where a comparably small $\varphi_1 = \pi/40$ is used, both partially centered B6 and full-bridge converters are noted to have the same ripple throughout the fundamental cycle. The same observation applies to Fig. 5(d), where a larger M_{ab} than M_{cb} has been used. Current ripple of the partially centered B6 converter will, in fact, only be higher when φ_1, M_{cb} or both are comparably high like in Fig. 5(b). As explained, the higher ripple is attributed to the lengthened T_1 and T_2 in Fig. 3(b) as φ_1 and M_{cb} increase. Regardless of that, ripple from the partially centered scheme is still smaller than that of the centered scheme discussed in Section III(A). The centered scheme will, in fact, match the partially centered scheme only when both φ_1 and M_{cb} are small like in Fig. 5(c).

IV. Discontinuous Modulation

Discontinuous modulation has been proposed for the B6 converter when it is used as a three-phase converter. Under balanced conditions, all three phases share the clamping equally, which means each phase will be clamped to either the upper or lower dc rail for 120°. Reduction in losses will then be spread among the three phases evenly. Such even spreading may however not be necessary when the B6 converter is used

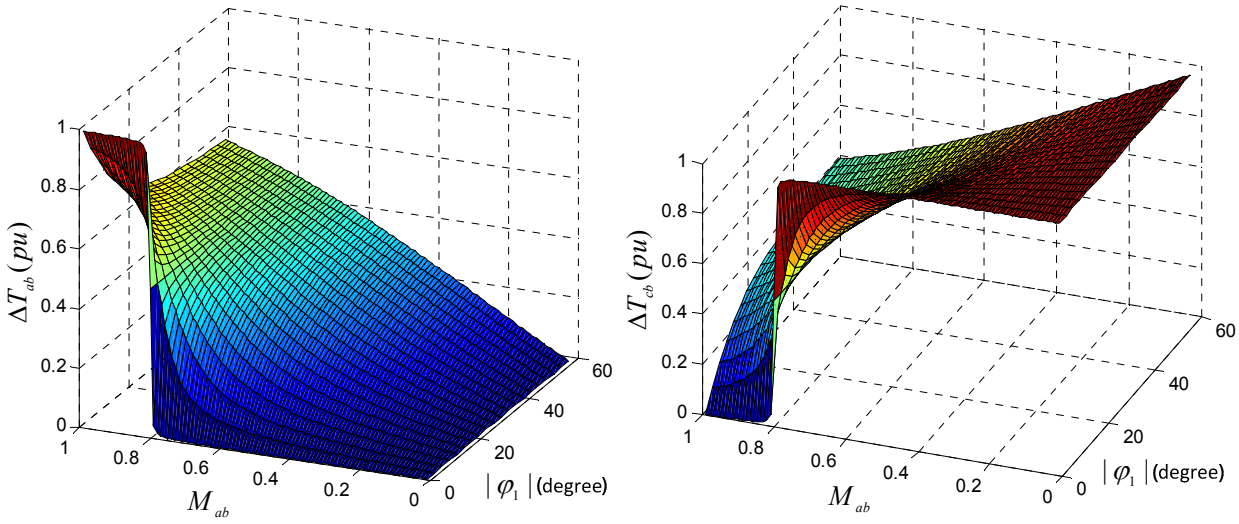

(a) (b)

Fig. 7. Clamping intervals (a) ΔT_{ab} and (b) ΔT_{cb} of the non-shared phase-legs as M_{ab} and φ_1 vary while keeping $M_{cb} = 0.8$.

as an asymmetrical single-phase converter with a shared phase-leg. This phase-leg carries the return currents of the other two non-shared phase-legs, which preferably, should cancel each other significantly. Else, the B6 converter may not be as attractive as two back-to-back full-bridges even though it uses two lesser switches. It is therefore reasonable to assume that current flowing through the shared phase-leg is much smaller with significantly lower losses generated. The clamping objective should hence tilt towards reducing losses from the two non-shared phase-legs rather than the shared phase-leg. Such clamping can be ensured by using offset and modulating references given in (11), where the minimum carrier peak needed is again equal to $M_{Tri,min}$ computed with (5). To avoid over-modulation, a small safety margin may also be added to get a slightly higher carrier peak M_{Tri}, which strictly, is a recommendation and not a necessary requirement.

$$\begin{cases} Ref_a^D = Ref_a + M_{off,D1} \\ Ref_b^D = Ref_b + M_{off,D1} \\ Ref_c^D = Ref_c + M_{off,D1} \end{cases}$$
$$M_{off,D1} = \begin{cases} sgn(Ref_a) * M_{Tri} - Ref_a, & if\ |Ref_a| \geq |Ref_c| \\ sgn(Ref_c) * M_{Tri} - Ref_c, & if\ |Ref_a| < |Ref_c| \end{cases},$$
$$M_{Tri} \geq M_{Tri,min} \qquad (11)$$

Considered an UPS with very close v_{ab} and v_{cb} [11], and a power ripple decoupling converter with v_{ab} and v_{cb} shifted by $\pi/4$ [16], applying (11) to them then results in Fig. 6(a) and (b), respectively. These figures clearly exhibit positive and negative clamping by the two non-shared phase-legs only, which certainly, is anticipated. Their intervals of clamping are also not always evenly distributed, and will vary with magnitude ratio $(M_{ab}: M_{cb})$ and phase-shift φ_1 between v_{ab} and v_{cb}. Expressions for computing them can be derived after determining t_1 and t_2, which according to Fig. 6(a) and (b), can be expressed as (12).

$$M_{ab}sin(\omega_1 t_1) = -M_{cb}sin(\omega_1 t_1 + \varphi_1)$$
$$\Rightarrow\ \omega_1 t_1 = tan^{-1}\left(\frac{-M_{cb}sin\varphi_1}{M_{ab}+M_{cb}cos\varphi_1}\right)$$
$$M_{ab}sin(\omega_1 t_2) = M_{cb}sin(\omega_1 t_2 + \varphi_1)$$
$$\Rightarrow\ \omega_1 t_2 = tan^{-1}\left(\frac{M_{cb}sin\varphi_1}{M_{ab}-M_{cb}cos\varphi_1}\right) \qquad (12)$$

Total positive and negative clamping time for the non-shared phase-leg linked to v_{ab} is then given by ΔT_{ab} in (13), which when subtracted from the fundamental period, gives the total clamping time ΔT_{cb} for the other non-shared phase-leg linked to v_{cb}.

$$\Delta T_{ab} = \begin{cases} 2(t_1 - t_2), & if\ t_1 \geq t_2 \\ 2(t_1 - t_2) + \frac{2\pi}{\omega_1}, & if\ t_1 < t_2 \end{cases} \Rightarrow$$
$$\Delta T_{ab} =$$
$$\begin{cases} \frac{2}{\omega_1}\left(tan^{-1}\left(\frac{-M_{cb}sin\varphi_1}{M_{ab}+M_{cb}cos\varphi_1}\right) - tan^{-1}\left(\frac{M_{cb}sin\varphi_1}{M_{ab}-M_{cb}cos\varphi_1}\right)\right), \\ \qquad if\ M_{ab} \leq M_{cb}|cos\varphi_1|,\ \varphi_1 \epsilon [0,\pi] \\ \frac{2}{\omega_1}\left(tan^{-1}\left(\frac{-M_{cb}sin\varphi_1}{M_{ab}+M_{cb}cos\varphi_1}\right) - tan^{-1}\left(\frac{M_{cb}sin\varphi_1}{M_{ab}-M_{cb}cos\varphi_1}\right)\right) + \frac{2\pi}{\omega_1}, \\ \qquad if\ M_{ab} > M_{cb}|cos\varphi_1|,\ \varphi_1 \epsilon [0,\pi] \end{cases}$$
$$\Delta T_{cb} = \frac{2\pi}{\omega_1} - \Delta T_{ab} \qquad (13)$$

Variations of ΔT_{ab} and ΔT_{cb} are plotted in Fig. 7 by varying $(M_{ab}: M_{cb})$ and φ_1, where $1pu = \frac{2\pi}{\omega_1}$. They will mostly be different except when $M_{ab} \approx M_{cb}$, at which, ΔT_{ab} and ΔT_{cb} are approximately equal regardless of how φ_1 varies.

V. Simulation and Experimental Results

Simulations and experiments have been performed with the B6 converter functioning as a simple single-phase ac-dc-ac converter shown in Fig. 8. At its input terminal is an ac source of v_{ab} = 110 V (RMS), which when rectified and controlled appropriately, provides a dc-link voltage of V_{dc} = 190 V. This dc-link voltage is, in turn, inverted to give an output voltage of v_{cb} = 110 V (RMS), but with a phase-shift of φ_l = π/4 introduced for better illustrating the intended voltage clamping. The output voltage is then applied to an ac filter and load combination consisting of L = 4.1 mH and R = 15 Ω, which in general, is fine for testing modulation concepts.

Frequencies of both input and output are also set to the same value of $\omega_l = 2\pi \times 50$ rad/s, which as explained earlier, permits a much smaller dc-link voltage to be used. This can be illustrated by referring to (1) and Fig. 1(b), which when implemented, requires a dc-link voltage of at least

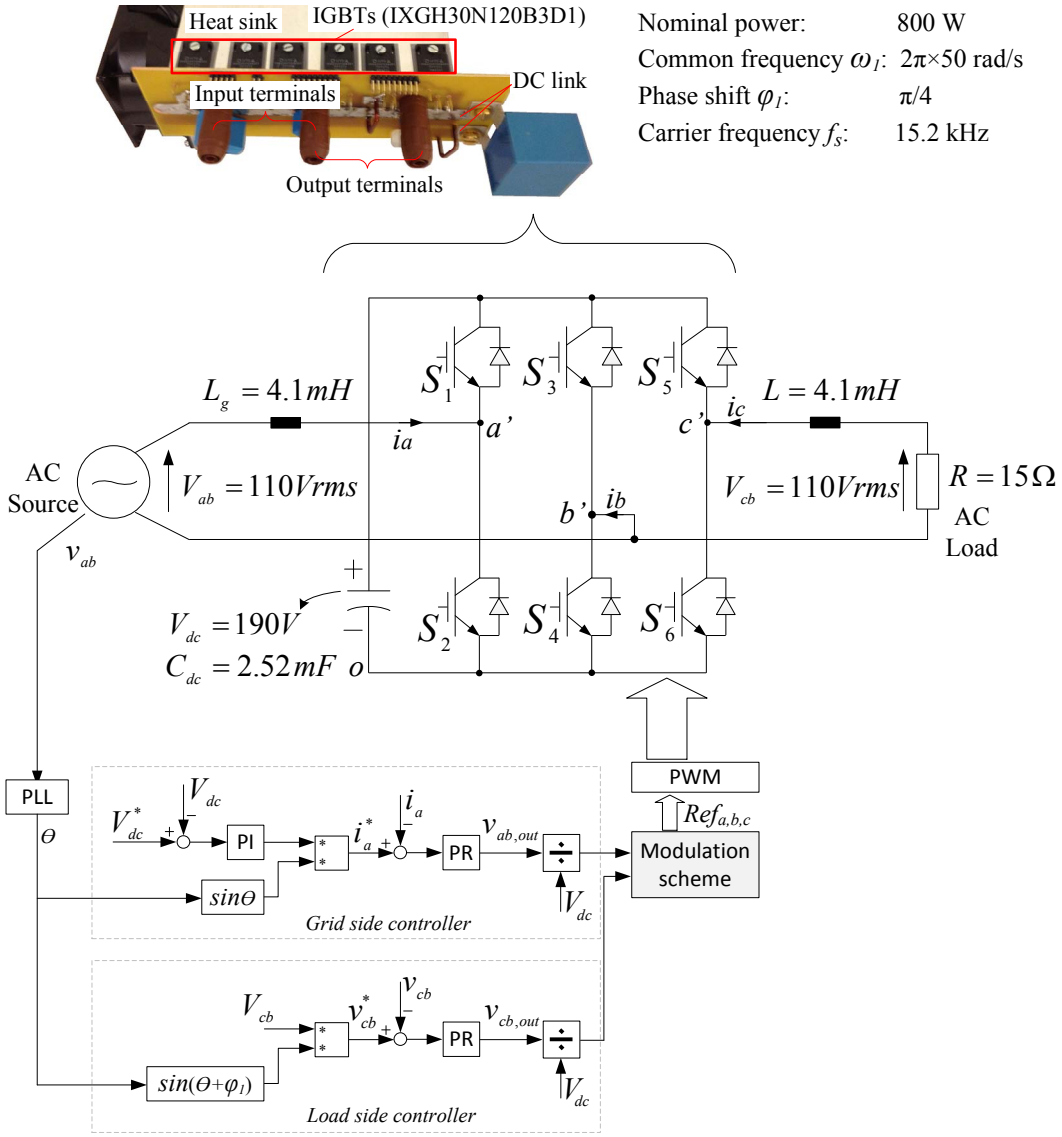

Fig. 8. The prototype and control diagram of the single-phase B6 converter for experiment.

$2 \times 110\sqrt{2} = 311$ V. On the other hand, the minimum dc-link voltage required by the proposed modulation schemes is 155.5 V, based on $M_{Tri,min}$ computed from (5). Inclusion of a safety margin to avoid over-modulation then results in the value of V_{dc} = 190 V chosen for testing. This value is still much smaller than that demanded by the scheme from (1). The setup is then operated with the three proposed modulation schemes applied in turn. Results obtained from them are described as follows

A. Continuous Modulation

Results obtained with the centered scheme from (2) and partially centered scheme from (7) are presented in Fig. 9 and Fig. 10, respectively. The centered scheme obviously switches all phase-legs continuously since its three modulating references are always centered within the carrier band without any clamping. Its accompanied current spectrum for i_a is plotted at the bottom of Fig. 9(b), which clearly, has a prominent harmonic cluster centered at the carrier frequency of 15.2 kHz. This cluster leads to a total harmonic distortion (THD) value of 2.9 % computed for i_a when modulated by the centered scheme from (2). On the other hand, the partially centered scheme has its harmonic cluster at 15.2 kHz reduced, which in terms of THD for i_a, gives a smaller value of 2.5 %. As explained, this improvement is introduced by centering the two preferred references rather than all three references.

Such centering may however lead to discontinuous clamping of the phase-leg modulated by the non-centered reference, which in Fig. 3(b), is $Ref_c^{C''}$. This clamping can clearly be seen in Fig. 10(a) and (b), which according to the loss distribution plots in Fig. 11, has helped to reduce switching losses from the clamped phase-leg. Loss distribution here is experimentally computed by measuring the individual switch currents and voltages at a high sampling rate, before multiplying them to obtain the switch losses offline. It should however be noted that clamping is not always introduced, and will, in fact, reduce to zero when magnitude of $Ref_c^{C'}$ in Fig. 3(b) falls below the carrier peak. When that happens, the first harmonic cluster in Fig. 10(b) will also reduce to zero since the two preferred references are now always centered.

This expectation can also be deduced from Fig. 5(c) and (d), where the magnitude of v_{cb} is comparably smaller than that of

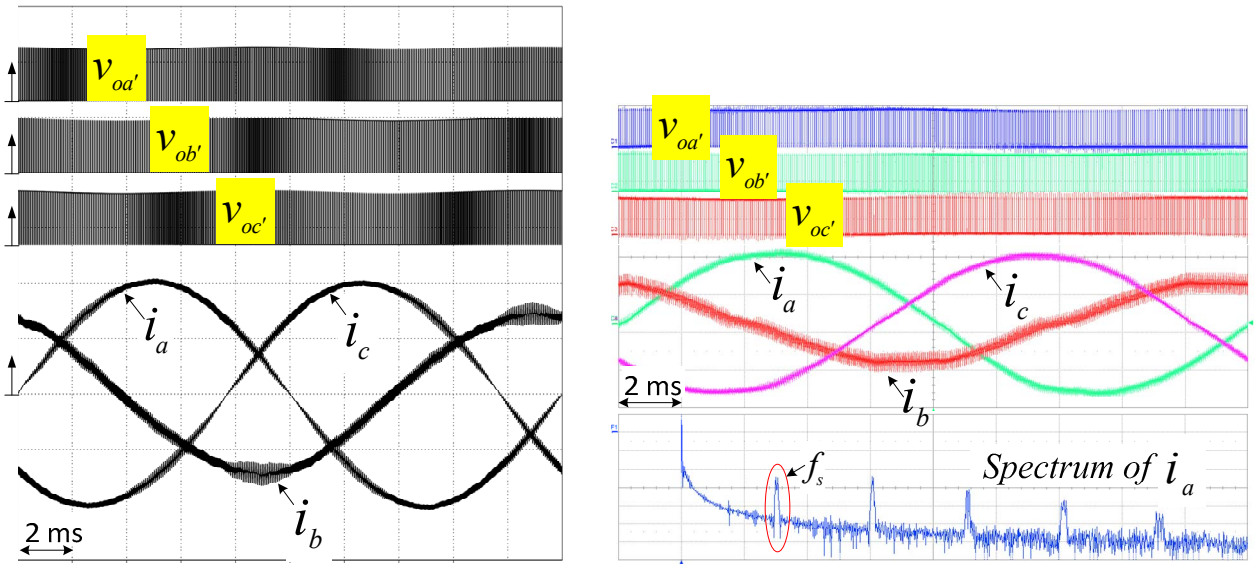

(a) Simulated (b) Experimental

Fig. 9. Waveforms of the B6 converter in Fig. 1(a) obtained with the centered scheme from (2) and $\varphi_1 = \pi/4$. ($v_{oa'}$, $v_{ob'}$, $v_{oc'}$: 200 V/div; i_a, i_b, i_c: 5 A/div; Spectrum: 10 dB/div, 10 kHz/div)

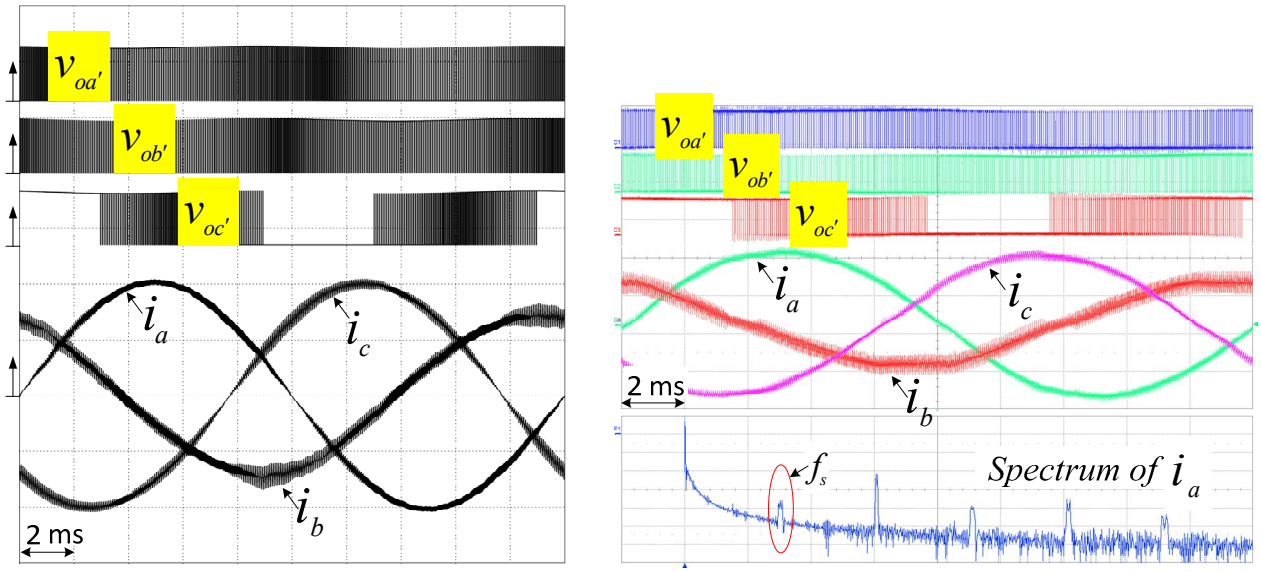

(a) Simulated (b) Experimental

Fig. 10. Waveforms of the B6 converter in Fig. 1(a) obtained with the partially centered scheme from (7) and $\varphi_1 = \pi/4$. ($v_{oa'}$, $v_{ob'}$, $v_{oc'}$: 200 V/div; i_a, i_b, i_c: 5 A/div; Spectrum: 10 dB/div, 10 kHz/div)

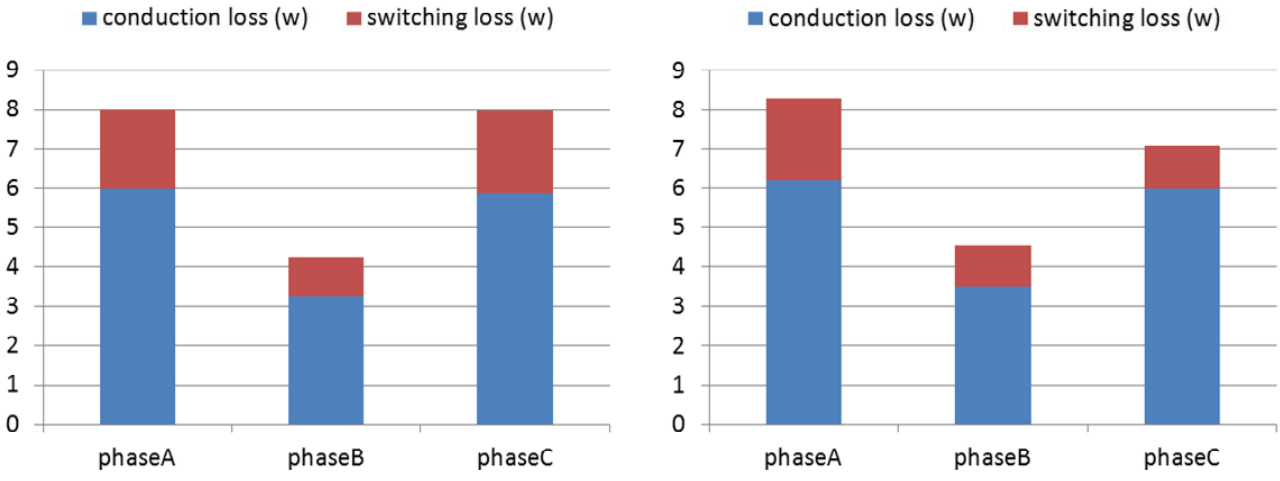

(a) (b)

Fig. 11. Experimental per-switch loss distributions of B6 converter when modulated by the (a) centered scheme from (2) and (b) partially centered scheme from (7).

Fig. 5(a) and (b). With their smaller v_{cb}, performance of the partially centered B6 converter in Fig. 5(c) and (d) is found to match exactly with that of a full-bridge converter implemented with four phase-legs for ac-dc-ac conversion. Since the spectrum of a full-bridge converter does not have a harmonic cluster at the carrier frequency of 15.2 kHz, the partially centered B6 converter will also not have component at the same frequency. It is therefore appropriate to say that the first harmonic cluster in Fig. 10(b) will eventually reduce to zero when $Ref_c^{C\prime}$ in Fig. 3(b) falls below the carrier peak.

B. Discontinuous Modulation

For easier comparison, simulation and experiment with the discontinuous scheme expressed in (11) are performed with the same parameters indicated in Fig. 8. Its captured results are shown in Fig. 12, where clamping of only the two non-shared phase-legs can clearly be seen. Such clamping shifts the modulating references away from the center of the carrier band, and hence a poorer THD of 3.9 % computed for i_a. The poorer current quality can also be seen from the larger first harmonic cluster at 15.2 kHz plotted at the bottom of Fig. 12(b). The discontinuous scheme however leads to the improved loss distribution shown in Fig. 13, which like Fig. 11 for the continuous schemes, is computed offline from experimentally measured switch voltages and currents sampled at a fast rate. In contrast, unlike Fig. 11, the distribution in Fig. 13 is obviously more uniform. The poorer i_a spectrum is therefore a tradeoff introduced by the lower total loss and improved loss distribution brought by the proposed discontinuous scheme.

C. Percentage Loss Comparison

Percentage loss generated by the B6 converter only without including the passive components can be computed by adding losses of all three phase-legs in either Fig. 11 or Fig. 13, and then dividing the sum by the nominal power of 800 W, as indicated in Fig. 8. The values computed are approximately 5.05 % ($=\frac{2\times(8+4.2+8)}{800}\times 100\%$) for the centered modulation scheme, 4.95 % for the partially centered scheme and 4.55 % for the discontinuous scheme. Efficiency of the B6 converter is then computed by subtracting the percentage loss from 100 %, which is close to 95 % for all three modulation schemes. A *Voltech PM3000A* meter is also used for measuring efficiency of the full experimental system including passive components indicated in Fig. 8. The values read are 89.3 % for the centered scheme, 89.6 % for the partially centered scheme and 90.1 % for the discontinuous scheme. These values are reasonable considering that the passive inductors have not been optimized.

In addition, it should be noted from Fig. 9, 10 and 12 that the return current i_b through the shared phase-leg is relatively significant for the system and parameters tested in Fig. 8. In cases where the return current can be reduced further, the converter efficiency will be raised further. This is especially true when i_a and i_c are close, which will then give a return current that is close to zero ($i_b = i_c - i_a \approx 0$). The B6 converter under those conditions will therefore likely be more efficient than two single-phase full-bridges connected back-to-back with the same dc-link voltage. The latter uses one additional phase-leg, and carries significant currents in all its phase-legs. It is therefore likely to be less efficient.

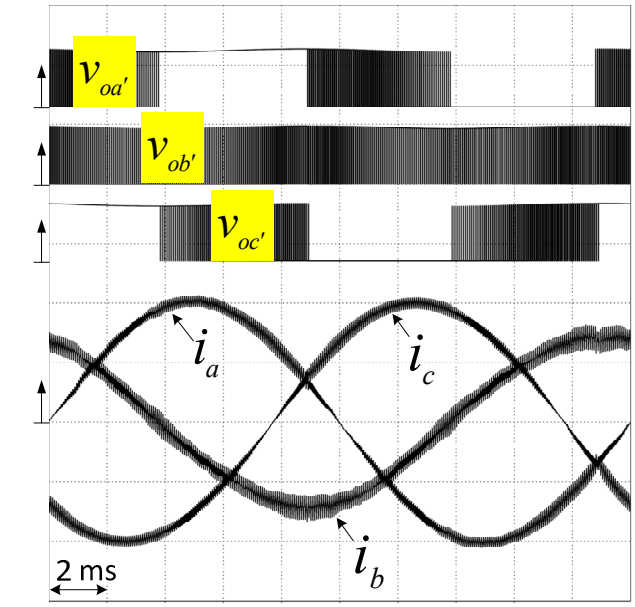

(a) Simulated

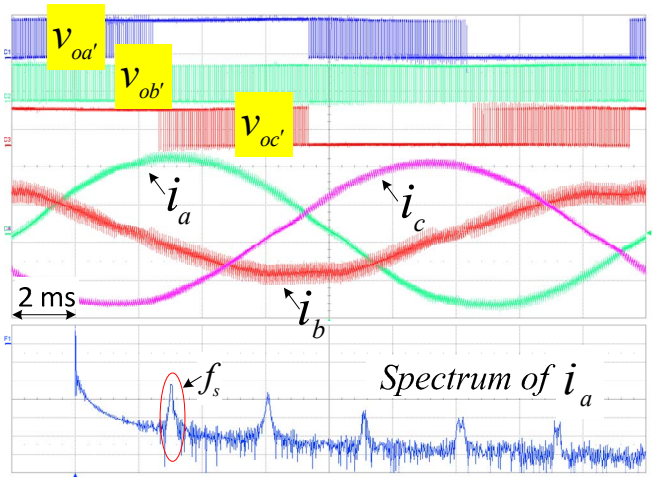

(b) Experimental

Fig. 12. Waveforms of the B6 converter in Fig. 1(a) obtained with the discontinuous scheme from (11) and $\varphi_1 = \pi/4$. ($v_{oa'}$, $v_{ob'}$, $v_{oc'}$: 200 V/div; i_a, i_b, i_c: 5 A/div; Spectrum: 10 dB/div, 10 kHz/div)

Fig. 13. Experimental per-switch loss distribution of B6 converter when modulated by the discontinuous scheme from (11).

VI. CONCLUSIONS

Continuous and discontinuous modulation schemes have been proposed for the B6 converter when used as a single-phase converter with two sets of ac terminals. The continuous centered scheme, in particular, helps to identify the minimum carrier peak needed for linear modulation, and hence the minimum dc-link voltage needed by the converter. The same minimum dc-link voltage can be ensured by the partially centered scheme, which instead of all references, centers only the two chosen references. Current flowing through phase-legs modulated by these two references will then have better spectral quality. The discontinuous scheme, on the other hand, has its loss distribution improved by clamping only the two non-shared phase-legs with higher losses. Losses of the three phase-legs are therefore brought closer at the expense of a poorer current quality when compared with the other two schemes. These different performance features have been observed in simulations and experiments, which indirectly, mean that the scheme chosen should be the one that better matches requirements of the application.

REFERENCES

[1] L. Zhong, M.F. Rahman, W.Y. Hu, K.W. Lim, "Analysis of direct torque control in permanent magnet synchronous motor drives," *IEEE Trans. Power Electron.*, vol. 12, no. 3, pp. 528-536, May 1997.

[2] A.D. Cheok, Y. Fukuda, "A new torque and flux control method for switched reluctance motor drives," *IEEE Trans. Power Electron.*, vol. 17, no. 4, pp. 543-557, Jul 2002.

[3] P. Rodríguez, A. Luna, R.S. Muñoz-Aguilar, I. Etxeberria-Otadui, R. Teodorescu, F. Blaabjerg, "A Stationary Reference Frame Grid Synchronization System for Three-Phase Grid-Connected Power Converters Under Adverse Grid Conditions," *IEEE Trans. Power Electron.*, vol. 27, no. 1, pp. 99-112, Jan. 2012.

[4] P. R. Martinez-Rodriguez, G. Escobar, A. A. Valdez-Fernandez, M. Hernandez-Gomez, J. M. Sosa, "Direct Power Control of a Three-Phase Rectifier Based on Positive Sequence Detection," *IEEE Trans. Ind. Electron.*, vol. 61, no. 8, pp. 4084-4092, Aug. 2014.

[5] R. J. Millnitz dos Santos, J. C. da Cunha, M. Mezaroba, "A Simplified Control Technique for a Dual Unified Power Quality Conditioner," *IEEE Trans. Ind. Electron.*, vol. 61, no. 11, pp. 5851-5860, Nov. 2014.

[6] H. Akagi, "New trends in active filters for power conditioning," *IEEE Trans. Ind. Appl.*, vol. 32, no. 6, pp. 1312-1322, 1996.

[7] M. H. Ahmet, J. K. Russel, L. A. Thomas, "Carrier-based PWM-VSI overmodulation strategies: analysis, comparison, and design," *IEEE Trans. on Power Electron.,* vol. 13, no. 4, pp. 674-689, 1998.

[8] H. W. van der Broeck, H. C. Skudelny, G. V. Stanke, "Analysis and realization of a pulsewidth modulator based on voltage space vectors," *IEEE Trans. on Industry Appl.,* vol. 24, no. 1, pp.142-150, 1988.

[9] K. Zhou, D. Wang, "Relationship between space-vector modulation and three-phase carrier-based PWM: a comprehensive analysis [three-phase inverters]," *IEEE Trans. on Ind. Electron.,* vol. 49, no. 1, pp. 186-196, 2002.

[10] D. G. Holmes, T. Lipo, "Pulse width modulation for power converters: principles and practice," John Wiley & Sons, 2003.

[11] D. Zhao, V.S.S.P.K. Hari, G. Narayanan, R. Ayyanar, "Space-Vector-Based Hybrid Pulsewidth Modulation Techniques for Reduced Harmonic Distortion and Switching Loss," *IEEE Trans. on Power Electron.*, vol. 25, no. 3, pp. 760-774, 2010.

[12] G. Narayanan, V. T. Ranganathan, D. Zhao, H. K. Krishnamurthy, R. Ayyanar, "Space Vector Based Hybrid PWM Techniques for Reduced Current Ripple," *IEEE Trans. on Ind. Electron.*, vol. 55, no. 4, pp. 1614-1627, April 2008.

[13] X. Mao, R. Ayyanar, H. K. Krishnamurthy, "Optimal Variable Switching Frequency Scheme for Reducing Switching Loss in Single-Phase Inverters Based on Time-Domain Ripple Analysis," *IEEE Trans. on Power Electron.*, vol. 24, no. 4, pp. 991-1001, April 2009.

[14] H.-W. Park, S.-J. Park, J.-G. Park, C.-U Kim, "A novel high-performance voltage regulator for single-phase AC sources," *IEEE Trans. on Ind. Electron.*, vol. 48, no. 3, pp. 554-562, 2001.

[15] J.-H. Choi, J.-M. Kwon, J.-H. Jung, B.-H. Kwon, "High-performance online UPS using three-leg-type converter," *IEEE Trans. Ind. Electron.*, vol. 52, no. 3, pp. 889-897, June 2005.

[16] N. Rocha, C.B. Jacobina, E.C. dos Santos, R.M.B. de Cavalcanti, "Parallel connection of two single-phase ac-dc-ac three-leg converter with interleaved technique," *in Proc. of IECON' 2012*, pp. 639 – 644, 2012.

[17] M. A. Vitorino, R. Wang, M. B. R. Correa, D. Boroyevich, "Compensation of DC-link oscillation in single-phase to single-phase VSC/CSC and power density comparison," *in Proc. of ECCE' 2012*, pp. 1121-1127, 2012.

[18] M. A. Vitorino, R. Wang, M. B. R. Correa, D. Boroyevich, "Compensation of DC-Link Oscillation in Single-Phase-to-Single-Phase VSC/CSC and Power Density Comparison," *IEEE Trans. on Ind. Appl.*, vol. 50, no. 3, pp. 2021 – 2028, 2014.

[19] H. Li, K. Zhang, H. Zhao, S. Fan, J. Xiong, "Active Power Decoupling for High-Power Single-Phase PWM Rectifiers," *IEEE Trans. on Power Electron.*, vol. 28, no. 3, pp. 1308-1319, 2013.

[20] K.-H. Chao, P.-T. Cheng, T. Shimizu, "New control methods for single phase PWM regenerative rectifier with power decoupling function," *in Proc. of PEDS' 2009*, pp. 1091-1096, 2009.

[21] S. Liang, X. Lu, R. Chen, Y. Liu, S. Zhang, F. Z. Peng, "A solid state variable capacitor with minimum DC capacitance," *in Proc. of APEC' 2014*, pp. 3496-3501, 2014.

[22] R. Chen, S. Liang, F. Z. Peng, "Generalized active power decoupling method for H-bridge with minimum voltage and current stress," *in the Proc. of ECCE' 2014*, pp. 4421-4427, 2014.

[23] S. Liang, F. Z. Peng, D. Cao, "A six-switch solid state variable capacitor with minimum DC capacitance," *in Proc. of ECCE' 2014*, pp. 4954-4959, 2014.

[24] A. Fatemi, M. Azizi, M. Mohamadian, A. Y. Varjani, M. Shahparasti, "Single-Phase Dual-Output Inverters With Three-Switch Legs," *IEEE Trans. on Ind. Electron.*, vol. 60, no. 5, pp. 1769-1779, 2013.

[25] A. Fatemi, M. Azizi, M. Mohamadian, F. Ashrafzadeh, "A minimized switch count single-phase AC/AC converter with active front end," *in Proc. of APEC' 2012*, pp. 1502 – 1507, 2012.

[26] X. Liu, P. Wang, P. C. Loh, F. Blaabjerg, M. Xue, "Six switches solution for single-phase AC/DC/AC converter with capability of second-order power mitigation in DC-link capacitor," *in Proc. of ECCE' 2011*, pp. 1368 – 1375, 2011.

Zian Qin (S'13) received his B.Eng and M.Eng from the Beihang University and Beijing Institute of Technology, Beijing, China, in 2009 and 2012, respectively. He is now working towards his Ph.D in Aalborg University, Aalborg, Denmark. In 2014, he was a Visiting Scientist with the Institute for Power Generation and Storage Systems (PGS), RWTH Aachen University, Aachen, Germany, where he focused on the wind power generation.

Poh Chiang Loh received his B.Eng (Hons) and M.Eng from the National University of Singapore in 1998 and 2000 respectively, and his Ph.D from Monash University, Australia, in 2002, all in electrical engineering. His interests are in power converters and their grid applications.

Frede Blaabjerg (S'86–M'88–SM'97–F'03) was with ABB-Scandia, Randers, Denmark, from 1987 to 1988. From 1988 to 1992, he was a Ph.D. Student with Aalborg University, Aalborg, Denmark. He became an Assistant Professor in 1992, an Associate Professor in 1996, and a Full Professor of power electronics and drives in 1998. His current research interests include power electronics and its applications such as in wind turbines, PV systems, reliability, harmonics and adjustable speed drives.

He has received 15 IEEE Prize Paper Awards, the IEEE PELS Distinguished Service Award in 2009, the EPE-PEMC Council Award in 2010, the IEEE William E. Newell Power Electronics Award 2014 and the Villum Kann Rasmussen Research Award 2014. He was an Editor-in-Chief of the IEEE TRANSACTIONS ON POWER ELECTRONICS from 2006 to 2012. He has been Distinguished Lecturer for the IEEE Power Electronics Society from 2005 to 2007 and for the IEEE Industry Applications Society from 2010 to 2011.